Conduction in Ionic Crystals

Anargha Mondal*[1]

[1]IISER Pune

August 6, 2025

Abstract

In this experiment we investigated the ionic conductivity of sodium chloride (NaCl) as a function of temperature. A cylindrical NaCl pellet was placed between brass electrodes in a high-temperature conductivity cell and heated in a muffle furnace up to about 700 °C. The current through the sample was measured at a fixed voltage while cooling, and the conductivity was calculated from the sample dimensions and electrode geometry. By plotting $\log_{10} K$ against $1/T$, we confirmed that NaCl exhibits Arrhenius-type behavior in the measured temperature range. We have obtained values of $E_a = 0.42740.0042$eV and $E_a = 0.670.011$eV for the cationic and anionic carriers, respectively, which average out to give $E_a = 0.560.013$eV for the entire temperature range. This result is consistent with the general range reported in the literature for ionic conduction in alkali halides, though slightly lower than the standard value for pure NaCl. The discrepancy is attributed to experimental limitations including contact resistance, temperature gradients, and the restricted range of intrinsic conductivity probed. The experiment demonstrates the temperature dependence of ionic conduction and provides a quantitative estimate of the activation energy governing ion transport in NaCl.

1 Introduction

Solids can be broadly classified by their electrical properties into conductors and insulators. Metals are good conductors and typically show a decrease in conductivity with increasing temperature, whereas ionic crystals such as alkali halides are insulators at room temperature and only become appreciably conductive at elevated temperatures. This contrasting behavior highlights that the charge carriers in ionic crystals differ from those in metals: in ionic crystals, current is carried not by free electrons but by the motion of ions themselves.

In sodium chloride (NaCl), the ions are normally locked in a highly ordered lattice. However, at temperatures above absolute zero, defects such as vacancies and interstitials are always present, and these allow ions to migrate. Under an applied electric field, diffusion of ions becomes biased in one direction, leading to ionic conduction. The number of mobile ions depends exponentially on temperature, as predicted by the Maxwell–Boltzmann distribution, which gives rise to an Arrhenius-type relation for the conductivity,

$$\log_{10} K \;\propto\; -\frac{E}{k_B}\,\frac{1}{T},$$

where E is the activation energy required for an ion to jump into a vacancy and participate in conduction.

Previous studies, such as those by Resoh and Hinrichen and more recent systematic measurements on pure and doped NaCl crystals [1], confirm that a plot of $\log_{10} K$ against $1/T$ is linear over appropriate temperature ranges, and the slope directly yields the activation energy. Reported values of E for NaCl are typically in the range 1.2–1.7 eV, depending on crystal purity, doping, and the conduction regime accessed.

The aim of the present experiment is to study ionic conduction in a NaCl pellet, to demonstrate experimentally that its conductivity increases with temperature, and to determine the activation energy from an Arrhenius analysis. By comparing the measured activation energy with literature values, I can assess the reliability of the experimental setup and discuss the limitations that affect accuracy.

*20221042

2 Theory

2.1 Explanation of ionic conduction in terms of the theory of lattice defects

We consider only one type of (stoichiometric) point defect: Schottky defect, whose number density are perfectly definite functions of the temperature. This is due to [2], where they have shown that for an analysis of conductivity in NaCl crystals, the regime of Frenkel defects need not be invoked.
In ionic crystals which possess Schottky defects there will be vacant anion lattice points and vacant cation lattice points. These are not independent, but must be equal in number to preserve electrical neutrality in the interior of the crystal. If W is the work necessary to remove an anion and cation from two distant points in the interior, and to incorporate them in new layers which are being built up on the surface of the crystal, then the number of (double) Schottky defects is:

$$n = N\gamma e^{-\frac{W}{2k_BT}}$$

where N is the total number of ion pairs and γ is the numerical factor arising from the change in the vibrational frequency of the atoms near the vacat lattice points. For simplicity, consider this effect to be small and $\gamma \approx 1$. There can be some instances when this formula breaks down, such as double hole dissociation, as discussed in [**?**].
Now if an electric field of strength $\vec{E}$ is applied, the probabilty per unit time that an ion moves in the direction of the field is:

$$\nu e^{-\frac{U-\frac{1}{2}eaE}{k_BT}}$$

where a is the crystal spacing, ν is the phonon mode frequency, and U is the height of the Coulomb barrier in the electron sea of the lattice. Similarly, in the opposite direction:

$$\nu e^{-\frac{U+\frac{1}{2}eaE}{k_BT}}$$

The mean drift velocity u is therefore, given by:

$$u = \nu a e^{-\frac{U}{k_BT}} 2sinh(\frac{1}{2}\frac{eEa}{k_BT}) \tag{1}$$

Since the fields used in practice $eEa << k_BT$, we may expand the last factor in (1). The conductivity due to one type of lattice defect is proportional to the number of these defects per cubic centimetre and to their mobility; both of these vary exponentially with the temperature; the conductivity thus takes the form:

$$K = K_0 e^{-\frac{\frac{1}{2}(W_0+U_0)}{k_BT}} \tag{2}$$

$$\tag{3}$$

where,

$$K_0 = (\gamma BC)\frac{Ne^2\nu a^2}{k_BT} \tag{4}$$

ν is the vibrational frequency, a the lattice constant, N th number of ion-pairs per cm^3, B is a measure of the activation energy to form a vacant site, and C is a measure of the self-diffusivity of the crystal. W_0 and U_0 are the We can reframe Eq. (2) to write:

$$\log K = \frac{E_a}{k_BT} \tag{5}$$

where, $E_a = \frac{W_0+U_0}{2}$ is the activation energy.

2.2 The anion migration problem in NaCl

Patterson, Rose, and Morrison [1] found an Arrhenius energy E_2 of 1.67 eV in the low-temperature regime; later Harrison, Morrison, and Rudham [2] found the Arrhenius plot of $logK$ against T^{-1} to comprise two parts, with a "knee" at about $500°C$. Lidiard [3] pointed out that this phenomenon could not correspond to diffusion by single vacancies since at low temperatures the naturally-occurring divalent cation impurity would depress the concentration of single anion vacancies, and suggested that this might be due to vacancy pairs at low temperatures ($< 500C$), and the "knee" indicates a regime change. Here, although our data shows this feature, we do not go into further analysis.

3 Experimental Apparatus

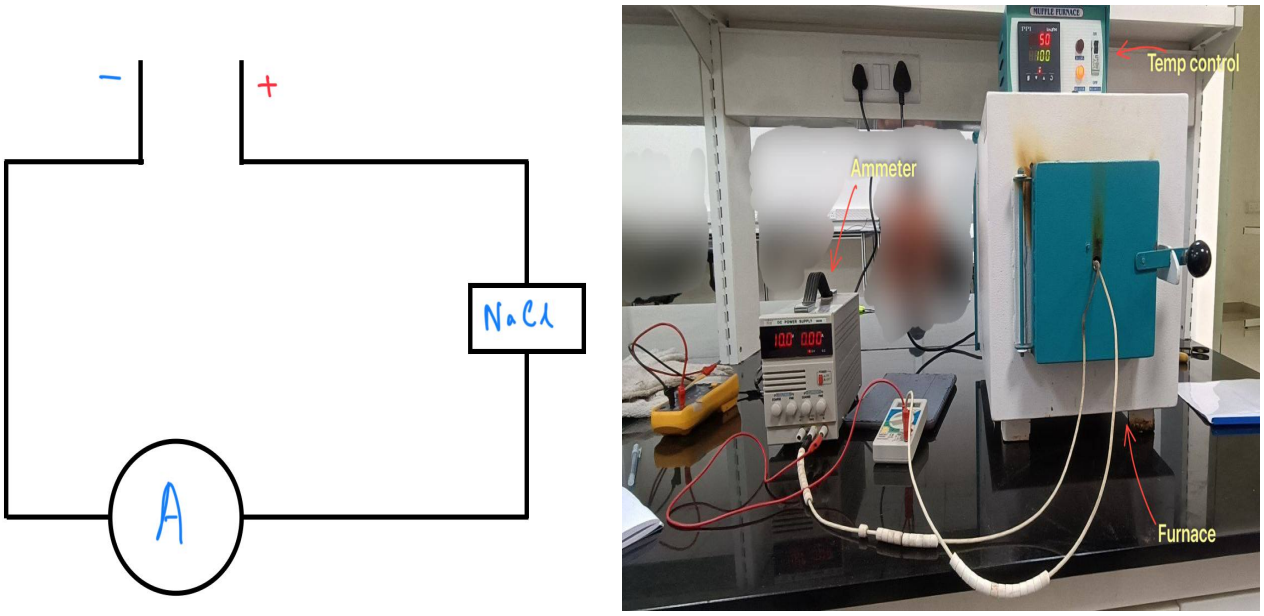

Figure 1: (*Left*) Circuit Diagram; (*Right*) Apparatus

The apparatus used in this experiment consisted of the following components:

1. **Ionic Conductivity Cell**
   The conductivity cell was designed to hold the NaCl sample pellet securely between two brass electrodes (B1 and B2). The electrodes were mounted on a frame constructed from Boller steel, chosen for its high melting point (1500 °C) and low coefficient of thermal expansion, allowing measurements up to ∼700 °C. The sample pellet, with a maximum height of 2 cm, was sandwiched between the electrodes. Electrical and thermal insulation was provided by marble tiles, which also supported the cell frame.

2. **Muffle Furnace**
   A muffle-type furnace capable of reaching temperatures up to 1000 °C was used to heat the sample. The sample cell was placed inside the furnace, with its marble tile covering the mouth of the furnace to minimize heat loss.

3. **Temperature Measurement**
   The furnace temperature was measured using a thermocouple, calibrated to directly display the temperature in degrees Celsius. The sample was positioned as close to the thermocouple as possible to ensure accurate temperature readings.

4. **Electrical Circuit**
   The following components were used to construct the measurement circuit:

   - Stable D.C. source: 10 V supply

- D.C. Voltmeter: Range 0–10 V
- D.C. Microammeter: Range 0–500 μA
- Variable Resistor: For controlling the applied current

The circuit allowed measurement of current through the sample at a fixed applied voltage as the temperature was varied.

5. **Sample**
   The specimen studied was a pellet of sodium chloride (NaCl), with a melting point of 804 °C. The pellet dimensions (diameter and height) were measured before the experiment to allow calculation of conductivity.

4 Data Collection

We write the conductivity as:

$$K = \frac{Ih}{VA} \tag{6}$$

where I gives the current through the sample, h and A give the thickness and area of cross-section of the crystal and V gives the voltage.

1. Measure the diameter and height of the NaCl pellet.
2. Place the pellet between the brass electrodes in the conductivity cell and tighten lightly.
3. Insert the cell into the furnace, ensuring proper thermal insulation with the marble tile.
4. Connect the circuit as per the schematic (D.C. source, voltmeter, microammeter, and variable resistor).
5. Switch on the furnace and gradually raise the temperature up to 700 °C.
6. At 700 °C, tighten the central rod slightly to improve electrical contact.
7. Record the current through the sample at a fixed applied voltage while the system cools, noting the corresponding temperatures from the thermocouple.

Measuring the dimensions of the crystal is important, and we have measured:

$$\boxed{h = 7.0 \pm 0.02mm; 2r = 13.46 \pm 0.02mm}$$

where h is the thickness of the crystal and r is the cross-sectional radius.

5 Results

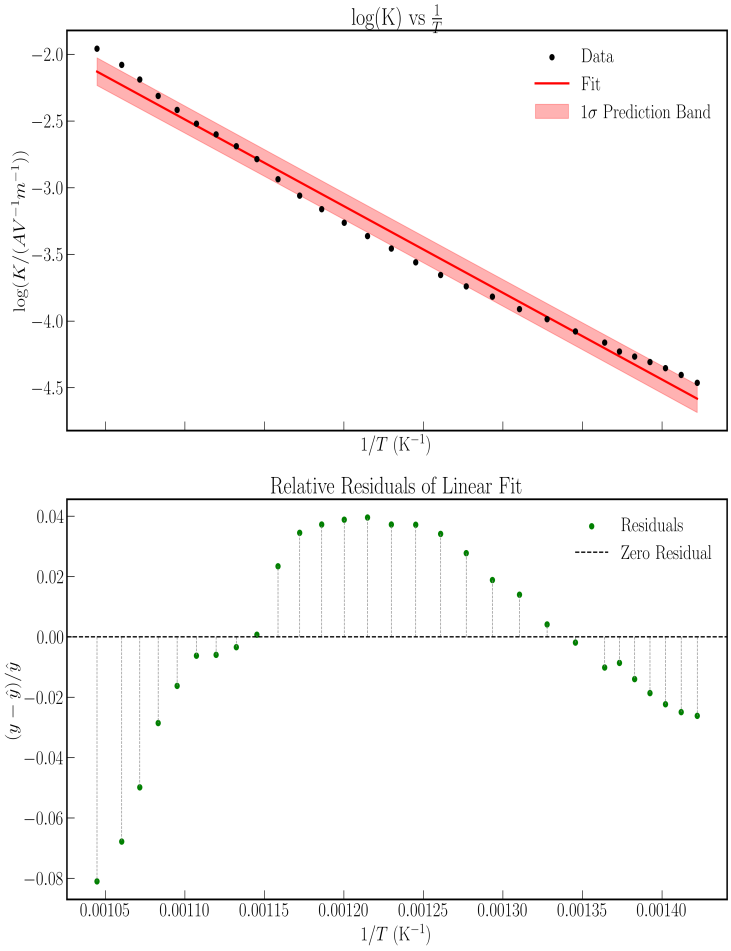

Figure 2: Fit of the entire plot, notice the knee

It is evident that we observe a "knee" in the (Arrhenius) plot at around $500°C$. This indicates a regime change in the transport properties, as has been mentioned earlier. Anhenius plots of the ionic conductivity of undoped NaCl in the form log K against T^{-1} display the typical segmented form characteristic of alkali halides with the "knee" at about $500°C$. However, the intrinsic region is remarkably straight with no evidence (to the eye) of any curvature, indicating either that the cation transport number is much greater than that of the anion, or that the Gibbs energies of migration of cation and anion vacancies must be very similar. The extrinsic part of the conductivity curve is also rather straight because of the low level of divalent cation impurity ($\sim$ 1 ppm) and the limited temperature range before the conductivity became too low to measure accurately.

Naively fitting the plot to find the activation energy E_a gives us a value of 0.57 eV, which does not quite capture the whole picture. The OLS fitting table in Table 1, sheds more light on this: However, it is more useful, if we simply fit the intrinsic regions for the two regimes separately. Proceeding as such we get $E_a^A = 0.44$ eV and $E_a^B = 0.7$ eV, where the regimes labeled A and B correspond to $T < 500°C$ and $T > 500°C$, respectively.

Table 1: OLS Regression Results

Dep. Variable:		y		**R-squared:**		0.986
Model:		OLS		**Adj. R-squared:**		0.985
Method:		Least Squares		**F-statistic:**		1881.
No. Observations:		29		**AIC:**		-51.92
Df Residuals:		27		**BIC:**		-49.18
Df Model:		1		**Covariance Type:**		nonrobust
	coef	**std err**	**t**	**P> |t|**	**[0.025**	**0.975]**
const	4.6589	0.186	25.050	0.000	4.277	5.040
x1	-6498.2835	149.842	-43.368	0.000	-6805.734	-6190.833

Omnibus:	5.201	**Durbin-Watson:**	0.072
Prob(Omnibus):	0.074	**Jarque-Bera (JB):**	1.774
Skew:	0.067	**Prob(JB):**	0.412
Kurtosis:	1.796	**Cond. No.**	8.44e+03

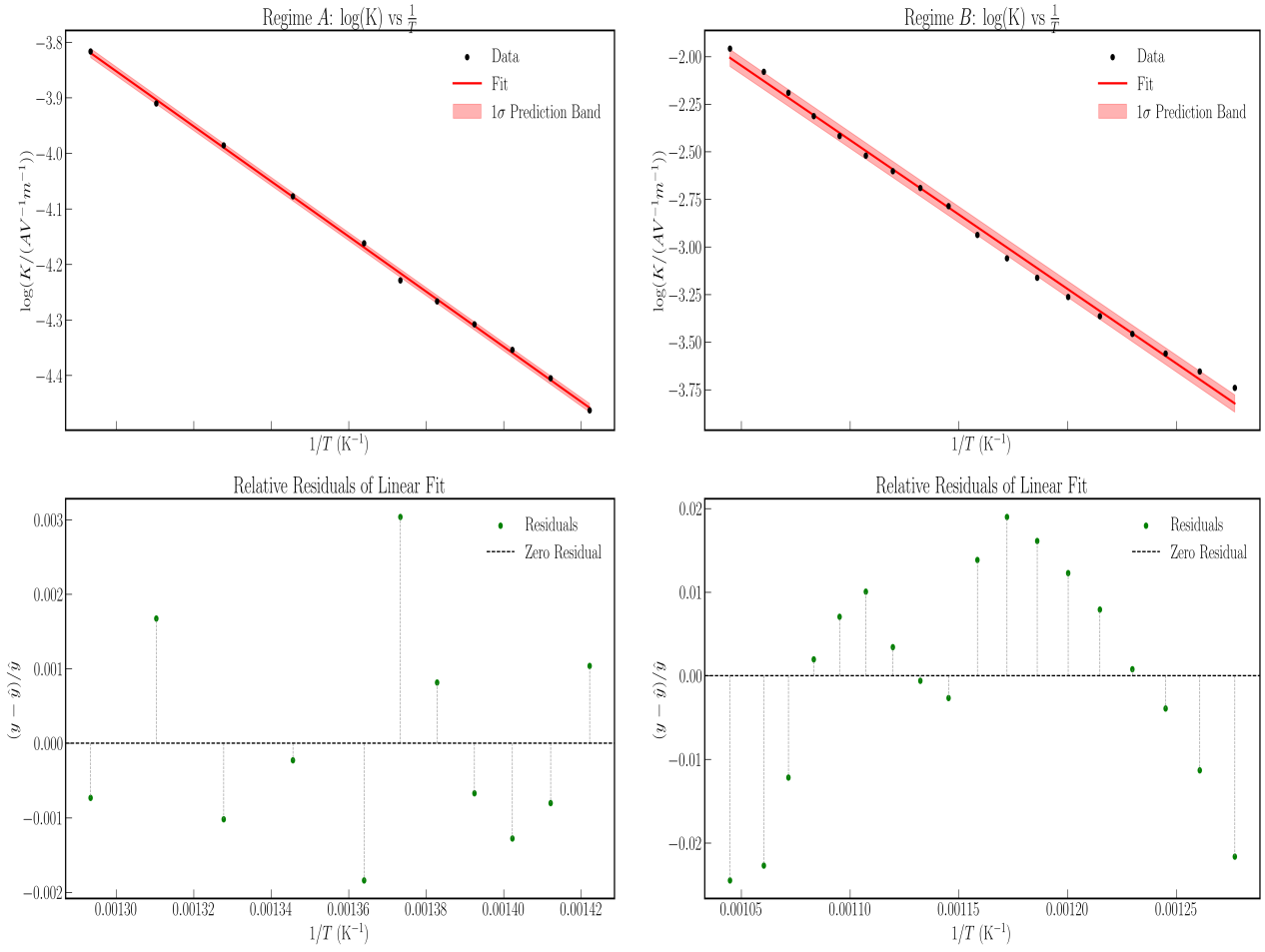

Figure 3: (*Left*)Fit for regime A ($T < 500°C$);(*Right*)Fit for regime B ($T > 500°C$

Notice that the activation energy for the cation vacancy migration enthalpy in the literature [1] is around 0.63 eV for pure NaCl, which is quite close to our value obtained in regime A, while the enthalpy of migration of anion vacancies is around 0.75 eV, which is quite similar to our activation energy for regime B. This precisely points to our phase transition anstatz, and tells us that **around** $500°C$**, the majority carriers change from cation vacancies to anion vacancies**. The following OLS fit table sheds some more light on this:

Regime A (Cation migration current)

Table 2: OLS Regression Results

Dep. Variable:		y		**R-squared:**		0.999
Model:		OLS		**Adj. R-squared:**		0.999
Method:		Least Squares		**F-statistic:**		1.053e+04
No. Observations:		11		**AIC:**		-77.90
Df Residuals:		9		**BIC:**		-77.10
Df Model:		1		**Covariance Type:**		nonrobust
	coef	**std err**	**t**	**P> |t|**	**[0.025**	**0.975]**
const	2.5979	0.066	39.311	0.000	2.448	2.747
x1	-4961.5231	48.357	-102.601	0.000	-5070.915	-4852.131

Omnibus:	2.183	**Durbin-Watson:**	2.338
Prob(Omnibus):	0.336	**Jarque-Bera (JB):**	1.195
Skew:	-0.790	**Prob(JB):**	0.550
Kurtosis:	2.666	**Cond. No.**	2.48e+04

Regime B (Anion migration current)

Table 3: OLS Regression Results

Dep. Variable:		y		**R-squared:**		0.995
Model:		OLS		**Adj. R-squared:**		0.995
Method:		Least Squares		**F-statistic:**		3435.
No. Observations:		18		**AIC:**		-63.37
Df Residuals:		16		**BIC:**		-61.59
Df Model:		1		**Covariance Type:**		nonrobust
	coef	**std err**	**t**	**P> |t|**	**[0.025**	**0.975]**
const	6.1651	0.155	39.897	0.000	5.838	6.493
x1	-7821.7304	133.459	-58.608	0.000	-8104.651	-7538.810

Omnibus:	0.910	**Durbin-Watson:**	0.330
Prob(Omnibus):	0.635	**Jarque-Bera (JB):**	0.825
Skew:	0.443	**Prob(JB):**	0.662
Kurtosis:	2.439	**Cond. No.**	1.43e+04

5.1 Error Analysis

We compute conductivity as

$$K = \frac{I\,h}{V\,A}, \qquad A = \frac{\pi d^2}{4},$$

where I is the measured current, V the applied voltage, h the pellet height and d the pellet diameter. For my sample We used $h = 7.00$ mm and $d = 13.46$ mm. Currents reported in the sheet (µA) were converted to A before computing K.

Uncertainty in the conductivity

Assuming independent uncertainties in We, V, h, d, the relative uncertainty in K is

$$\left(\frac{\sigma_K}{K}\right)^2 = \left(\frac{\sigma_I}{We}\right)^2 + \left(\frac{\sigma_h}{h}\right)^2 + \left(\frac{\sigma_V}{V}\right)^2 + \left(\frac{\sigma_A}{A}\right)^2, \qquad \frac{\sigma_A}{A} = 2\frac{\sigma_d}{d}.$$

Consequently (and because We use base-10 logarithms),

$$\sigma_{\log_{10} K} = \frac{1}{\ln 10}\,\frac{\sigma_K}{K}.$$

For the full fit

Refering to Table 1, we have:
The parameter of interest is the coefficient of x_1 (the slope):

$$m = -6.498283473250421 \times 10^3, \qquad \sigma_m = 149.8421668 \quad (1\text{–}\sigma \text{ standard error}).$$

Substituting the numbers for E_a (for the full temperature range):

$$E_a = (6.498283473250421 \times 10^3) \times (1.38 \times 10^{-23}) \times (6.242 \times 10^1 8) = 0.56 \text{ eV}.$$

Uncertainty on E_a. Evidently, the uncertainty propagates linearly:

$$\sigma_{E_a} = (149.8421668) \times (1.38 \times 10^{-23}) \times (6.242 \times 10^{18}) = 0.013 \text{ eV}.$$

Thus

$$\boxed{E_a = 0.56 \pm 0.013 \text{ eV}}$$

avergaed over both the regimes. The $1-\sigma$ limits have been highlighted in Figure 2.

For Regime A (Cationic vacancy carriers)

From the OLS regression of $\log_{10} K$ versus $1/T$ we obtained the slope

$$m = -4961.5231, \qquad \sigma_m = 48.3574 \quad (1\sigma).$$

The activation energy for the cationic carriers

$$E_a^{\text{cations}} = (4961.5231) \times (1.38 \times 10^{-23}) \times (6.242 \times 10^{18}) = 0.4274 \text{ eV},$$

with uncertainty

$$\sigma_{E_a^{\text{cations}}} = (48.3574) \times (1.38 \times 10^{-23}) \times (6.242 \times 10^{18}) = 0.0042 \text{ eV}.$$

Thus

$$\boxed{E_a^{\text{cations}} = 0.4274 \pm 0.0042 \text{ eV}}.$$

for the cationic carriers.

For Regime B (Anionic vacancy carriers)

The activation energy for the anionic carriers

$$E_a^{\text{anionic}} = (7821.7304) \times (1.38 \times 10^{-23}) \times (6.242 \times 10^{18}) = 0.67 \text{ eV}.$$

The propagated uncertainty (treating f as exact) is

$$\sigma_{E_a^{\text{anionic}}} = (133.45894578) \times (1.38 \times 10^{-23}) \times (6.242 \times 10^{18}) = 0.011 \text{ eV}.$$

Thus

$$\boxed{E_a^{\text{anions}} = 0.67 \pm 0.011 \text{ eV}}$$

for the anionic carriers

Remarks on uncertainties and systematics

- The quoted uncertainty on E above is the statistical uncertainty derived from the linear fit (slope standard error). We did not inflate uncertainties by instrument specifications unless explicitly supplied.
- Systematic effects that can bias E include contact resistance between pellet and electrodes, temperature gradients across the pellet, thermocouple calibration error, and leakage currents. These were not fully propagated into the numerical uncertainty above; to include them one should (i) estimate each systematic (e.g., contact resistance as an equivalent series resistance vs. temperature), (ii) convert into an effective change in $\log_{10} K$ vs. $1/T$, and (iii) combine in quadrature with the statistical error or report separately.
- Because $1/T$ (the x-axis) has finite uncertainty from thermocouple precision and gradients, a more rigorous treatment would use an errors-in-variables method (orthogonal distance regression). The result above uses ordinary least squares on $\log_{10} K$ vs $1/T$ and the fit covariance to estimate the slope uncertainty.

6 Limitations and Sources of Error

In carrying out this experiment, we list the limitations that affect the accuracy and scope of the results:

- **Temperature gradients:** The thermocouple reading did not always reflect the exact temperature of the pellet. The sample may have been slightly cooler or hotter than the indicated value due to gradients in the furnace.
- **Contact resistance:** The interface between the NaCl pellet and the brass electrodes introduced additional resistance.
- **Sample brittleness:** The NaCl pellet became brittle after repeated heating and cooling, raising the possibility of micro-cracks which would alter the effective cross-sectional area.
- **Limited voltage range:** Since the applied voltage was fixed at 10 V, we could not probe whether the conductivity showed non-linear effects with field strength.
- **Data resolution:** The microammeter and thermocouple had finite precision, which limited the resolution of my data, especially at low currents near the lower end of the temperature range.
- **Narrow intrinsic region:** Due to instrumental sensitivity, we could not access a wide range of the intrinsic conductivity regime before the currents became too small to measure reliably.

7 Conclusions and Discussion

We have obtained values of $E_a = 0.42740.0042$eV and $E_a = 0.670.011$eV for the cationic and anionic carriers, respectively, which average out to give $E_a = 0.560.013$eV for the entire temperature range. These are quite concordant with literarture values ([1], [2])The first conclusion to be drawn from the computer analysis of these conductivity data is that the Schottky defect model is adequate for NaCl. Our results do not prove that Frenkel defects do not form in NaCl, but they do show that it is not necessary to include cation and/or anion Frenkel defects in fitting the conductivity.
More solid confirmation of the conclusions of this work will be obtained, however from (1) studies of transmission electron microscopy in which the colloids can be most directly observed, and (2) studies of thermal conductivity at even lower temperature, where the dominant phonons will have wavelengths much larger than the particle size.

References

[1] Hooton & Jacobs, Ionic Conductivity of Pure and Doped Sodium Chloride Crystals, 1987, Canadian Journal of Chemistry

[2] Worlock, J.M., Thermal Conductivity in Sodium Chloride Crystals Containing Silver Colloids, Physical Review, 1966

[3] Electronic Processes in Ionic Crystals, Mott & Gurney, 1946 Reprint.

[4] IISER Pune Physics Lab 5 Manual

Appendix

Collected Raw Data

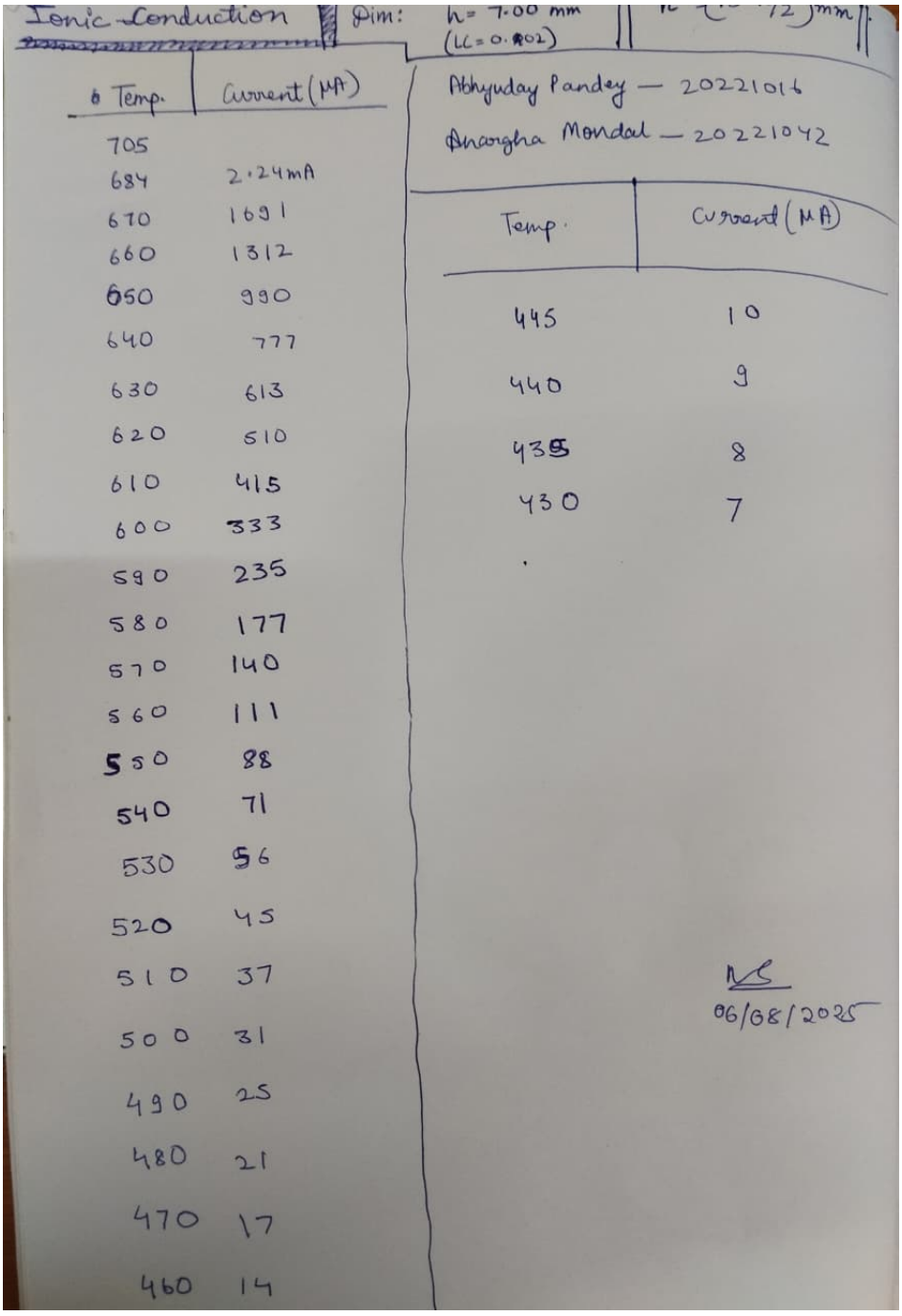

Ionic Conduction Dim: h = 7.00 mm (LC = 0.002)

Abhyuday Pandey — 20221016

Anargha Mondal — 20221042

Temp.	Current (μA)
705	
684	2.24mA
670	1691
660	1312
650	990
640	777
630	613
620	510
610	415
600	333
590	235
580	177
570	140
560	111
550	88
540	71
530	56
520	45
510	37
500	31
490	25
480	21
470	17
460	14

Temp.	Current (μA)
445	10
440	9
435	8
430	7

06/08/2025